Hindawi Publishing Corporation
Journal of Nanomaterials
Volume 2013, Article ID 473703, 6 pages
http://dx.doi.org/10.1155/2013/473703

Research Article

DNA Detection of *Toxoplasma gondii* with a Magnetic Molecular Beacon Probe via CdTe@Ni Quantum Dots as Energy Donor

Shichao Xu,[1,2] Chen Zhang,[1] Lei He,[1] Tongyao Wang,[1] Liusong Ni,[1] Mengna Sun,[1] Heng Miao,[1] Jimei Zhang,[1,2] Zhao Dai,[1,2] Bing Wang,[1,2] and Guo Zheng[1]

[1] *State Key Laboratory of Hollow Fiber Membrane Materials and Membrane Process, Tianjin Polytechnic University, Tianjin 300382, China*
[2] *School of Environmental and Chemical Engineering, Tianjin Polytechnic University, Tianjin 300382, China*

Correspondence should be addressed to Shichao Xu; xushichao@tjpu.edu.cn

Received 24 March 2013; Accepted 14 June 2013

Academic Editor: Sebastian Mackowski

A new method for detection of *Toxoplasma gondii* via DNA sensing technology was developed in this study. It was based on the mechanism of fluorescence resonance energy transfer (FRET) in which multifunctional and magnetic-fluorescent CdTe@Ni quantum dots (mQDs) were utilized as energy donor and a commercial BHQ_2 as acceptor. The sensing probe was fabricated by labeling a stem-loop *Toxoplasma gondii* DNA oligonucleotide with CdTe@Ni mQDs at the 5′ end and BHQ_2 at 3′ end, respectively. The surface assembly of CdTe on Ni core and the formation of CdTe@Ni were confirmed by XRD analysis. The sizes of CdTe, Ni nanoparticles, and CdTe@Ni were measured via TEM and XRD methods and estimated to be ~3 nm, ~15 nm, and ~20 nm, respectively. The sensing ability was investigated by the fluorescence spectrum (FS). An obvious fluorescence recovery was observed when the complete complimentary target *Toxoplasma gondii* DNA was introduced, which did not happen in the case of the target DNA with one-base pair mismatch. Our research indicates that the current sensing probe is sensitive and specific in detection of *Toxoplasma gondii* DNA and has great potential in Toxoplasmosis diagnosis.

1. Introduction

In the past decades, one of the most prominent and fastest moving interfaces of nanotechnology was the synthesis and application of semiconductor nanomaterials (such as quantum dots (QDs)) in biological detection and bioimaging [1–10]. The QDs have preeminent photophysical and chemical properties [11]: (1) efficient quantum yield, high brightness, and stability of the QDs against photobleaching; (2) the luminescence properties of QDs, which can be controlled by size due to the quantum confinement; (3) the luminescence spectra of QDs that reveal narrow emission bands and large Stokes shifts; (4) in contrast to organic fluorophores or transition metal complexes that exhibit broad absorbance bands and require specific wavelength excitation, QDs can be excited by a common high-energy excitation wavelength, leading to the size-controlled luminescence. Biological detection of fluorescent probes was based on fluorescence resonance energy transfer (FRET) mechanism [12], and QDs were used as an energy donor due to their excellent fluorescent properties. The molecular beacon sensing probe based on FRET was usually applied in DNA detection, in which the donor and acceptor were connected by a typical DNA strand with a stem-loop beacon structure. The FRET efficiency was controlled by altering the distance between the energy donor and acceptor [13].

Toxoplasma gondii is an obligate intracellular protozoan parasite belonging to the phylum Apicomplexa, subclass Coccidia. *Toxoplasma gondii* infections are known almost worldwide, and around one-third of the world's population is seropositive for this parasite. The infections of many Asians, including Chinese, were also reported [14]. The efficient technology and early detection of *Toxoplasma gondii* or its shedding oocysts are necessary. Traditional method to detect

Table 1: The DNA sequences in experiment.

Nomenclature	Sequence
Molecular beacon probe	5′-NH_2-$(CH_2)_6$-AGCTATTATAAACTCGTTGGATGCATAGCT-3′-BHQ2
Mismatch sequence	5′-TGCATCCAATGAGTTTATAA-3
Complementary sequences	5′-TGCATCCAACGAGTTTATAA-3

the *Toxoplasma gondii* or diagnosis of Toxoplasmosis was time consuming and required professional knowledge. In current research, we developed a magnetic sensing probe for fast, convenient, and efficient analysis of *Toxoplasma gondii* DNA by using CdTe@Ni magnetic nanoparticles (MNPs) as an energy donor. Our data indicated that the target *Toxoplasma gondii* DNA could be successfully detected by the sensing probe.

2. Materials and Methods

2.1. Apparatus. The UV-vis absorption spectra were obtained in the range of 450–700 nm on Thermo Spectronic Corp. model Helios-γ. Fluorescence spectra were measured by F-380 fluorospectrophotometer (Tianjin Gangdong Scientific and Technical Development Co. Ltd., China) under ambient temperature with excitation slit of 10 nm, emission slit width of 8 nm, and photomultiplier tube voltage of 100 V. Zeta potential of CdTe QDs and Ni NPs was analyzed using nano-Zeta potential and submicron particle size analyzer (Beckman Coulter, Inc., USA) with laser source of 7 mW@655 nm and sonication power of 80 W@36 kHz, and the measurement was performed under ambient condition. Morphology properties were analyzed on transmission electron microscopy ((TEM); Tecnai 20 G2 S-TWN, FEI Co., USA), and samples for all of these TEM experiments were prepared by dispersing the as-prepared samples in ethanol, sonicating for 2 min to ensure adequate dispersion of the nanostructures on lacey carbon covered Cu grid. X-ray powder diffraction (XRD) investigation was carried out via D/Max-IIA diffractometry (Rigaku, Japan) using Cu-K radiation (50 kV, 100 mA).

2.2. Materials. Te powder was obtained from Delan Fine Chemicals Co. Ltd. (Tianjin, China), and $NiCl_2$ and $CdCl_2$ were obtained from Sino-reagent Co. Ltd. (Shanghai, China). Mercaptopropionic acid (MPA) was purchased from Sigma-Aldrich (USA). DNA sequences, derived from *Toxoplasma gondii*, and 1-ethyl-3-(dimethylaminopropyl) carbodiimide hydrochloride (EDC) were purchased from Shanghai Invitrogen Biotechnology Co. Ltd. (Shanghai, China). All the chemicals used are of analytical grade without further purification. Ultrapure water and N_2 were used throughout experiments. The DNA sequences from *Toxoplasma gondii* in the experiment were indicated in Table 1.

2.3. Synthesis of CdTe Quantum Dots. The CdTe was synthesized in aqueous phase according to the previous recipe described by Sarah et al. in 2011 [15] with some modifications. Briefly, $CdCl_2$ and MPA were mixed with mole ratio of 1 : 3 and adjusted the pH value to be 9.0. The prepared precursor NaHTe solution was added and refluxed for 5 h at 10°C. By altering the refluxing time, QDs with different emission colors were prepared.

2.4. Preparation of CdTe@Ni Nanoparticles. Typically, CdTe@Ni NPs were prepared via the reduction method with hydrazine hydrate, as previously reported [16]. Nickel chloride ($NiCl_2{\cdot}6H_2O$) and sodium hydroxide were added into ethylene glycol phase at 60°C for 0.5 h. Ni nanoparticles were magnetically precipitated and washed several times with ultrapure water and acetone. The resulting Ni nanoparticles were surfacely modified with 1,6-hexamethylenediamine (pH = 3.0), followed by adding CdTe QDs (mole ratio of Ni : CdTe was 1 : 9). The reactant solution was refluxed at 45°C for 0.5 h, and MNPs were achieved.

2.5. Fabrication of Molecular Beacon (MB) Probe. The MB probe was obtained by reacting with 0.5 mL the as-prepared CdTe@Ni solution, 20 μL probe DNA, 0.5 mL EDC, and 980 μL phosphate buffers ((PBS), pH = 8.2) at ambient temperature for 24 h.

2.6. Detection of Target DNA. 100 μL target DNA and 2.0 mL sensing probe DNA were added into a 5 mL penicillin bottle which contained 0.5 mL of 20 mM Tris-HCl buffer. The hybridization reaction happened at 37°C for 2 h.

3. Results and Discussion

3.1. Characterizations of CdTe QDs. The prepared CdTe QDs expressed excellent optical properties such as strong fluorescence intensity (FI), narrow emission peak, and broad UV absorption. Figures 1(a) and 1(b) were the fluorescence spectrum (FS) and UV-vis absorption spectrum, respectively. The emission colors varied from blue to red with the increase of emission wavelength (Figure 1(a)). Therefore, CdTe QDs refluxed for 4 h was used throughout the experiment due to its good fluorescent properties. The size of the synthesized CdTe was calculated using the polynomial fitting function [17]:

$$D = \left(9.8127 \times 10^{-7}\right)\lambda^3 - \left(1.7147 \times 10^{-3}\right)\lambda^2 + (1.0064)\,\lambda - 194.84, \quad (1)$$

where the λ is the absorption maxima of the QDs. And the diameter of CdTe (4 h) was 2.6 nm. The concentration of CdTe QDs solution was 1.29×10^{-6} M, determined via Lambert-Beer's law [18]. The corresponding fluorescence quantum yields (Φ_F) were estimated according to [19]:

$$\Phi_F = \Phi_s \left(\frac{F}{F_s}\right)\left(\frac{A_s}{A}\right)\left(\frac{n^2}{n_s^2}\right), \quad (2)$$

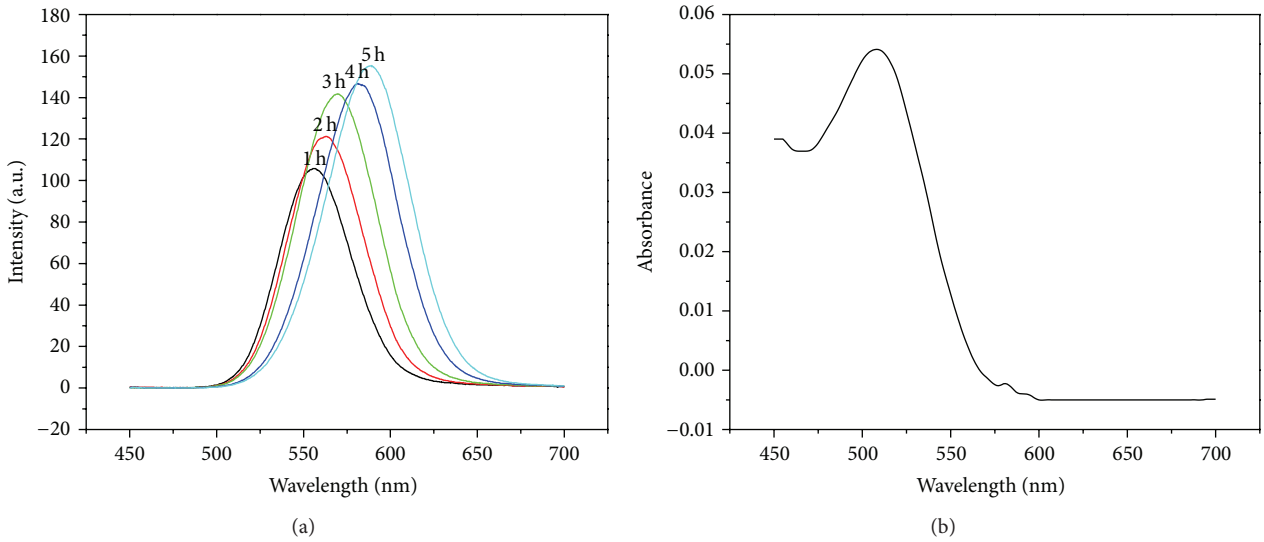

Figure 1: The fluorescence spectrum of CdTe QDs (a) and UV-vis absorption spectrum of CdTe (4 h) (b), $\lambda = 512$ nm.

where A and A_s were the absorbance of the sample and standard at the excitation wavelength, respectively. F and F_s were the areas under the fluorescence curves of the QDs and standard, respectively. n and n_s are the refractive indices of the solvent used for the sample and standard, respectively. Rhodamine 6 G in ethanol ($\Phi_s = 0.95$) was used as the standard [16]. Then, the calculated value of Φ_F was 27.3%.

CdTe QDs were further characterized by transmission electron microscopy (TEM) (shown in Figure 2). TEM data indicated that the CdTe QDs had a favorable dispersity, and the size was ca. 3.0 nm according to theoretical calculated value.

3.2. Characterizations of CdTe@Ni NPs. The prepared Ni magnetic nanoparticles (MNPs) were characterized by X-ray diffraction (XRD) (Figure 3) and TEM (Figure 4(a)). The size of Ni MNPs was determined to be 10.5 nm, based on XRD analysis and the Scherrer equation [19]. The average size of Ni MNPs analyzed by TEM was 13.0 nm, and obvious agglomeration phenomenon of Ni MNPs was observed (Figure 4(a)). However, after the Ni MNPs was further modified by 1,6-hexamethylenediamine, the modified Ni MNPs had a better dispersity than before, and the average size was about 20.0 nm (Figure 4(b)). It confirmed that 1,6- hexamethylenediamine played a crucial role in reducing agglomeration.

The modified MNPs were further characterized by Zeta potential analysis. The Zeta potential value was 5.67 as shown in Figure 5, which means that particle surface was electropositive. This result indicated the successful surface modification of 1,6-hexamethylenediamine, which was good for CdTe@Ni synthesis.

The prepared CdTe@Ni was characterized with TEM (Figure 6) and XRD (Figure 7). The diameter of CdTe@Ni was uniform and estimated to be ca. 35.0 nm (Figure 6). The increase of 20 nm in diameter was observed compared with the Ni (15 nm), which indicates that the CdTe was successfully capped on the Ni core. Little agglomeration was observed

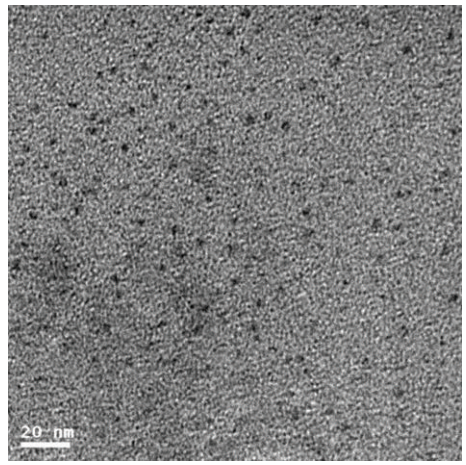

Figure 2: TEM image of the prepared CdTe QDs.

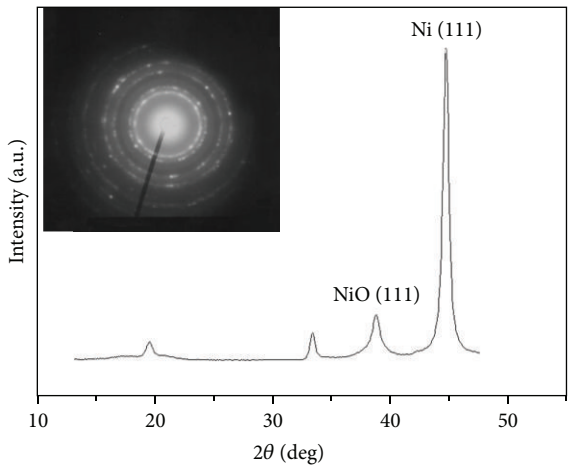

Figure 3: XRD pattern and selected area electron diffraction (inner graph) of Ni MNPs.

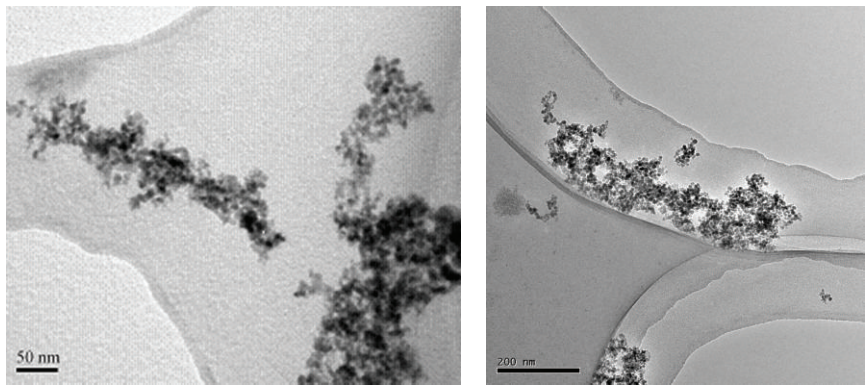

(a) (b)

Figure 4: TEM images of Ni MNPs (a) and modified Ni MNPs (b).

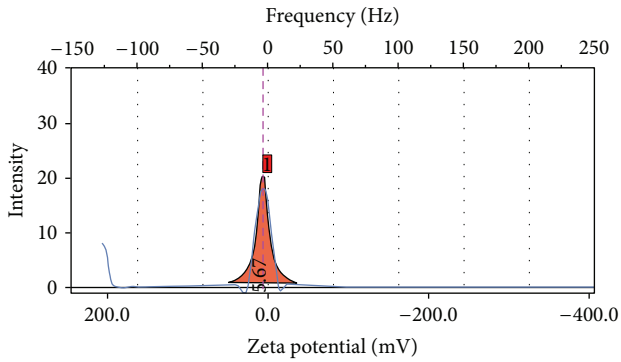

Figure 5: Zeta potential analysis of modified Ni MNPs.

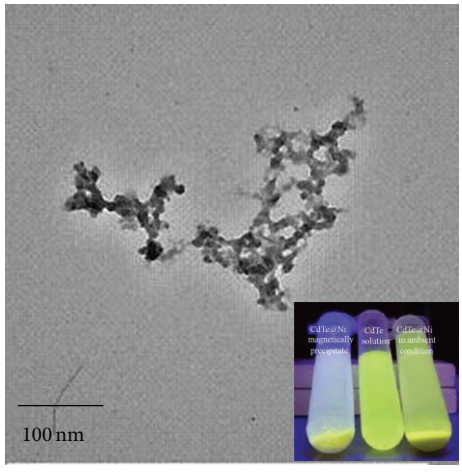

Figure 6: TEM image of CdTe@Ni nanoparticles.

due to the magnetism of CdTe@Ni. Moreover, the greenish CdTe@Ni was suspended well in aqueous solution and conveniently precipitated by a common magnet (Figure 6, inner graph).

XRD patterns in Figure 7 indicate that the intensity of NiO (111) and Ni (111) was obviously decreased after formation

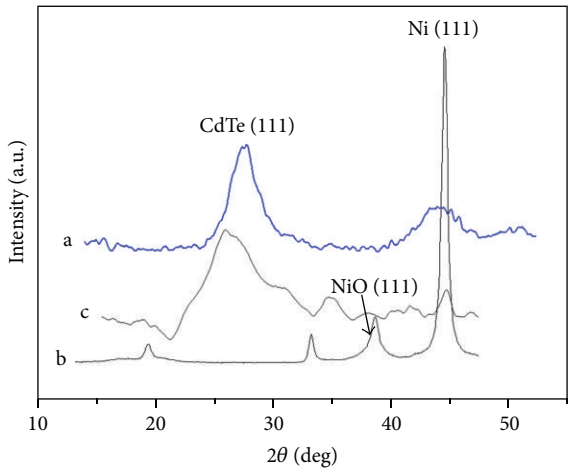

Figure 7: XRD patterns of CdTe QDs (a), Ni MNPs (b), and CdTe@Ni QDs (c).

of CdTe shell on the Ni particle core, which indicates that CdTe@Ni QDs was successfully achieved.

3.3. Sensitivity and Specificity of Prepared MB Probe. About 56% of CdTe@Ni FI was decreased by comparing peak 1 and peak 3 as shown in Figure 8(a), which indicated that the MB probe was successfully created when using CdTe@Ni as energy donor and BHQ_2 as acceptor. However, the data in Figure 2(a) peak 3 showed low FI of the MB probe (commonly named as background noise) since the expiated energy from CdTe@Ni donor was not completely quenched by the BHQ_2. It may involve the following possibilities. Firstly, the fluorescence emission spectra of CdTe@Ni donor and the UV absorption spectrum of BHQ_2 were not perfectly overlapped after formation of the core-shell structure (which usually causes the size change of donor), and the fluorescence emitted by the donor was not completely absorbed, thus showing a certain degree of fluorescence. Secondly, compared with the small organic molecules BHQ_2, CdTe@Ni with greater surface area had more trap states, resulting in the emission energy not totally going to be absorbed by the acceptor. The

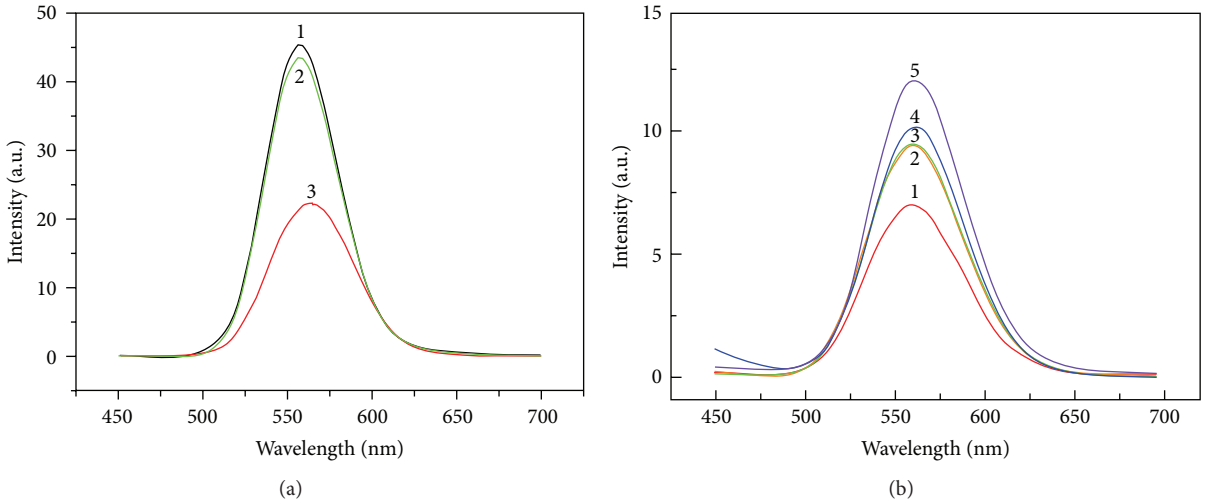

FIGURE 8: (a) The FS of molecular beacon sensing system. Target DNA; line 1: CdTe@Ni solution, line 2: MB solution after adding target DNA, and line 3: MB solution. (b) The FS of FRET after adding various target DNA; line 1: MB solution without target DNA, line 2 to line 4: adding target DNA with one mismatch, and line 5: adding completely complementary target DNA of *Toxoplasma gondii*.

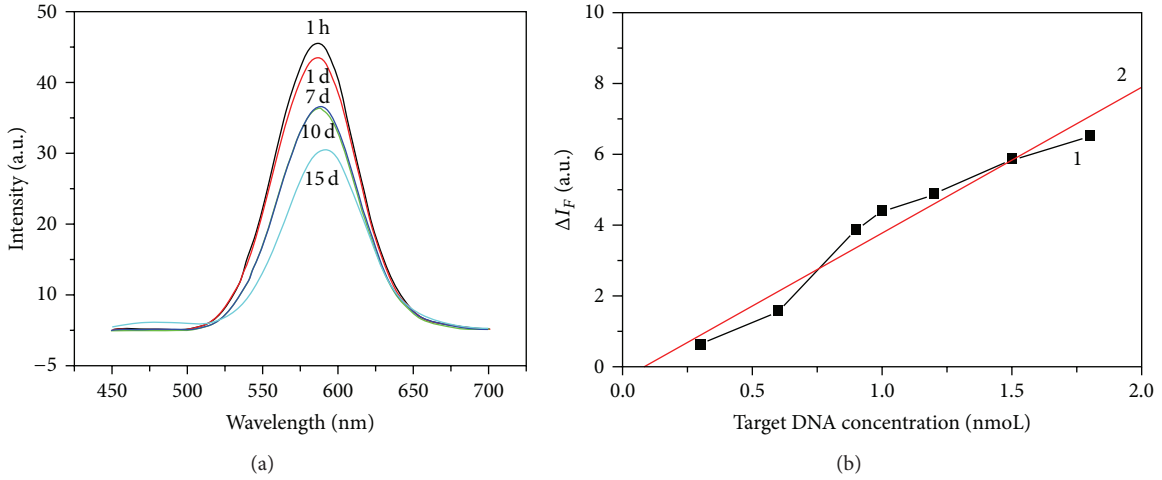

FIGURE 9: (a) Stability investigation of MB probe via FS. (b) Standard curve of detection of the target DNA.

FI was thoroughly recovered after adding the complementary target DNA, which revealed that the DNA sensing system had excellent sensitivity.

A mathematic modeling and practical method were proposed in our later research to reveal the possible factors that caused and decreased the noise, and the data will be reported elsewhere. Currently, the MB solution was diluted 4 times to decrease the effect of background noise for investigating the specificity. The obvious differences in the fluorescence intensity recovery (FR) were confirmed when different target DNA was applied in MB sensing probe solution. Compared with the complementary DNA (Figure 8(b), peak 5), the one-base mismatched DNA (Figure 8(b), peak 2 to peak 4) resulted in a much lower FR. This clearly demonstrates the excellent specificity of molecular beacons in detecting *Toxoplasma gondii* DNA. The difference in the MB hybridization between perfectly matched and single-base mismatched DNA relies on the stability of the newly formed DNA duplexes. Length of the hybridization sequence, location of mismatch bases in the sequence, and hybridization temperature have effects upon duplex stability. Therefore, high specificity with one-base mismatch DNA identification capability can be obtained by using carefully designed molecular beacon probes and optimized hybridization conditions.

FI was gradually reduced with the time-elapsing, and 30% of FI disappeared after 15 days of storage. The red-shift of emission peak was observed simultaneously. However, long-term stability is expected for the further applications, and the MB probe can be stabilized at 4°C for one month under the light-shielding condition. The MB limit of detection (LOD) was investigated via calibration curve (Figure 9) and calculated to be 2.70×10^{-9} mol/L.

4. Conclusion

The CdTe@Ni nanoparticles with magnetic and fluorescent properties were synthesized and successfully used in molecular beacon (MB) probes as energy donors in *Toxoplasma gondii* DNA detection. The resulting data demonstrated that the sensing probe was sensitive, rapid, and specific in detecting the *Toxoplasma gondii* target DNA. This study indicates that the sensing probe has great potentials in early detection of Toxoplasmosis.

Acknowledgment

The current research was funded by Tianjin National Science Foundation of China (no. 11JCZDJC22300 and no. 13JCQNJC02600).

References

[1] Y. Wang, R. Hu, G. Lin et al., "Functionalized quantum dots for biosensing and bioimaging and concerns on toxicity," *ACS Applied Materials & Interfaces*, vol. 5, no. 8, pp. 2786–2799, 2013.

[2] A. M. Smith and S. Nie, "Semiconductor nanocrystals: structure, properties, and band gap engineering," *Accounts of Chemical Research*, vol. 43, no. 2, pp. 190–200, 2010.

[3] X. Chi, D. Huang, Z. Zhao, Z. Zhou, Z. Yin, and J. Gao, "Nanoprobes for in vitro diagnostics of cancer and infectious diseases," *Biomaterials*, vol. 33, no. 1, pp. 189–206, 2012.

[4] A. Mandal, J. Nakayama, N. Tamai, V. Biju, and M. Isikawa, "Optical and dynamic properties of water-soluble highly luminescent CdTe quantum dots," *Journal of Physical Chemistry B*, vol. 111, no. 44, pp. 12765–12771, 2007.

[5] G. Jiang, A. S. Susha, A. A. Lutich, F. D. Stefani, J. Feldmann, and A. L. Rogach, "Cascaded FRET in conjugated polymer/quantum dot/dye-labeled DNA complexes for DNA hybridization detection," *ACS Nano*, vol. 3, no. 12, pp. 4127–4131, 2009.

[6] Y. Li, L. Liu, X. Fang, J. Bao, M. Han, and Z. Dai, "Electrochemiluminescence biosensor based on CdSe quantum dots for the detection of thrombin," *Electrochimica Acta*, vol. 65, pp. 1–6, 2012.

[7] D. Chen, G. Wang, and J. Li, "Interfacial bioelectrochemistry: fabrication, properties and applications of functional nanostructured biointerfaces," *Journal of Physical Chemistry C*, vol. 111, no. 6, pp. 2351–2367, 2007.

[8] Z. Deng, Y. Zhang, J. Yue, F. Tang, and Q. Wei, "Green and orange CdTe quantum dots as effective pH-sensitive fluorescent probes for dual simultaneous and independent detection of viruses," *Journal of Physical Chemistry B*, vol. 111, no. 41, pp. 12024–12031, 2007.

[9] K. E. Sapsford, T. Pons, I. L. Medintz et al., "Kinetics of metal-affinity driven self-assembly between proteins or peptides and CdSe-ZnS quantum dots," *Journal of Physical Chemistry C*, vol. 111, no. 31, pp. 11528–11538, 2007.

[10] S. C. Xu, M. Heng, Y. Q. Yang et al., "Fluorescence enhanced quantum dots: its synthesis, optical properties, and ecotoxicity research," *Advanced Materials Research*, vol. 152-153, pp. 208–211, 2011.

[11] R. Freeman, J. Girsh, and I. Willner, "Nucleic acid/quantum dots (QDs) hybrid systems for optical and photoelectrochemical sensing," *ACS Applied Materials & Interfaces*, vol. 5, no. 8, pp. 2815–2834, 2013.

[12] G. Chen, F. Song, X. Xiong, and X. Peng, "Fluorescent nanosensors based on Fluorescence Resonance Energy Transfer (FRET)," *Industrial & Engineering Chemistry Research*, 2013.

[13] C.-W. Chi, Y.-H. Lao, Y.-S. Li, and L.-C. Chen, "A quantum dot-aptamer beacon using a DNA intercalating dye as the FRET reporter: application to label-free thrombin detection," *Biosensors and Bioelectronics*, vol. 26, no. 7, pp. 3346–3352, 2011.

[14] P. Zhou, H. Zhang, R.-Q. Lin et al., "Genetic characterization of *Toxoplasma gondii* isolates from China," *Parasitology International*, vol. 58, no. 2, pp. 193–195, 2009.

[15] D. Sarah, A. Edith, and N. Tebello, "Synthesis and photophysical studies of CdTe quantum dot-monosubstituted Zinc phthalocyanine conjugates," *Inorganica Chimica Acta*, vol. 367, pp. 173–181, 2011.

[16] I. Caraman, G. I. Rusu, and L. Leontie, "The photoluminescence of CdTe thin films in SnO_2-CdS/CdTe-Ni solar cells thermally treated in $CdCl_2$ solution," *Journal of Optoelectronics and Advanced Materials*, vol. 9, no. 5, pp. 1546–1550, 2007.

[17] S. D'Souza, E. Antunes, and T. Nyokong, "Synthesis and photophysical studies of CdTe quantum dot-monosubstituted zinc phthalocyanine conjugates," *Inorganica Chimica Acta*, vol. 367, no. 1, pp. 173–181, 2011.

[18] T. Toyo'oka, H. P. Chokshi, R. G. Carlson, R. S. Givens, and S. M. Lunte, "Oxazole-based tagging reagents for analysis of secondary amines and thiols by liquid chromtography with fluorescence detection," *Analyst*, vol. 118, no. 3, pp. 257–263, 1993.

[19] G. Krishnamurthy and R. Viswanatha, "Tunable infrared phosphors using Cu doping in semiconductor nanocrystals: surface electronic structure evaluation," *The Journal of Physical Chemistry Letters*, vol. 4, pp. 409–415, 2013.